BULGARIAN ACADEMY OF SCIENCES
“ACAD. ROSTISLAW KAISCHEW’’ INSTITUTE OF PHYSICAL CHEMISTRY
DEPARTMENT OF INTERFACES AND COLLOIDS

Nikolay Nedialkov Panchev

# A Method for electromicrointerferometric studies of water-in-oil emulsion films: development and applications

SUMMARY

4.2 Chemical sciences (Physical chemistry)

Scientific supervisor: assoc. prof. Khristo Khristov
Scientific consultant: acad. Dotchi Exerowa

Sofia, 2022

The thesis contains 152 pages, 84 figures, tables and illustrations. Total of 159 literature sources are quoted.

Numbering of the chapters, figures and tables in the summary is identical with the numbering in the thesis.

# Introduction

One of the main problems encountered during the crude oil production is the formation of undesired water-oil-water emulsions. The major industrial goal is the destruction of these emulsions for to achieve reasonable phase separation of water and oil. It is generally recognized that the thinning of emulsion films and their resistance to rupture play a crucial role in determining the stability of emulsions. Studies of film drainage and rupture are believed to provide an insight to actual mechanisms underlying droplet–droplet coalescence, not well understood as yet. To break a stable emulsion film, an external force has to be applied to the film. The applied excess force will be counteracted by the disjoining pressure in order to maintain film integrity. Once the external force exceeds the disjoining pressure, the film will drain and eventually rupture. Such an excess force can be either mechanical capillary pressure or an electrical force from an electric field applied across the film. In fact, one of the most preferred industrial methods for destabilizing petroleum emulsions is application of external DC fields.

Detailed information derived from quantitative studies of emulsion films is still surprisingly scarce. It may be said though that certain stirring in that direction is on the verge of becoming noticeable, evidenced also with the new methods and techniques developed in the recent years.

## Structure of the thesis

The thesis contains ten chapters. First four of them comprise the literature overview. Chapter 1 describes the formation and the nature of petroleum emulsions. Chapter 2 is focused on the stability of these emulsions and the role of thin liquid films in petroleum studies. Chapter 3 presents different industrial means for breaking petroleum emulsions with the emphasize on electrical methods. Chapter 4 is dedicated to theoretical and experimental studies on the mechanisms of forced rupture of bulk dielectric layers, thin liquid films and bilayer lipid membranes. Then the experimental part follows, starting with the defining the goal of dissertation, development of the experimental methodology and the choice of used materials. Chapters 5-10 describe the experimental results and their analysis. The dissertation concludes with the prospects for the future applications of the proposed experimental method and with the list of main contributions.

# Chapter 5. Experimental setup and materials

## 5.1 Goal

During the upstream production of crude oil it is common that both type of emulsions are formed, namely water-in-oil (w/o) and oil-in-water (o/w), Picture 5.1. In w/o emulsions the oil is the continuous phase, while aqueous droplets are the dispersed phase. Usually the w/o emulsions are more stable and represent the main challenge for phase separation in the petroleum industry. The main question thus is how to remove the water?

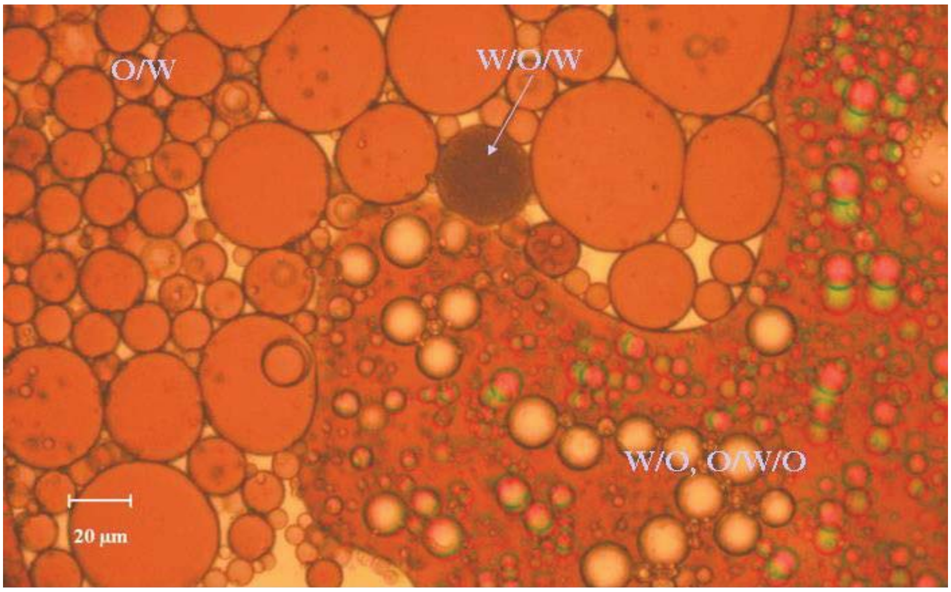

Picture 5.1. Formation of real coexisting water-in-oil and oil-in-water emulsions [Syncrude Ltd]

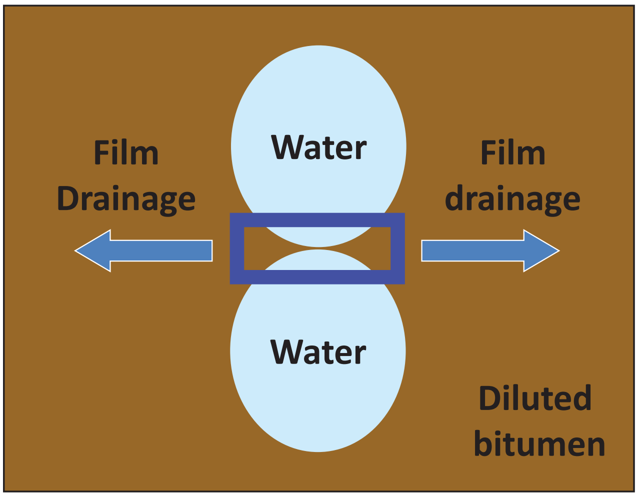

Figure 5.1. Schematic of the formation of oil film between two aqueous droplets in contact.

As already mentioned in the literature overview, the importance of film research follows from the fact that film stability in large extent determines the emulsion stability, which in turn determines the industrial froth treatment (phase separation) performance.

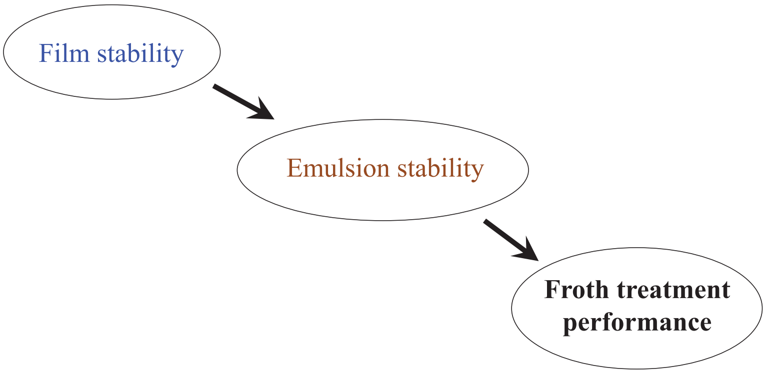

**The goal** of this thesis was to develop a new method to study water-in-oil emulsion single films that combines AC or DC polarization with the optical microinterferometry. For this purpose a new measuring cell was designed as well as the upgradement of the Thin Liquid Film – Pressure Balance Technique (TLF-PBT).

The three main objectives of applying the new technique were: i) to measure critical voltage of rupture and to demonstrate that it can be used as parameter describing film stability, ii) to study the effect of film size on electro-induced rupture, iii) to obtain film capacitance.

### 5.2 Development of the electro-microinterferometric method

Studies of water-in-oil emulsion films are limited. Particularly in presence of applied external electric fields, there is only one study by Anklam et al. However, Anklam's method does not allow independent determination of film parameters as well as the true disjoining pressure (instead they measure "pseudo pressure"). The major advantage of suggested new technique is that within a single film specimen it is possible to determine independently the most important film parameters both by microinterferometry and electrical measurements:

- Film diameter (in micro-meter range),
- Film thickness (in nano-meter range),
- Rate of film drainage (nm/sec),
- Film lifetime,
- Critical DC voltage of film rupture, $V_{cr}$

- Effect of applied electric field on surface forces (true disjoining pressure isotherms),
- Film capacitance and relative film permittivity (AC voltage).

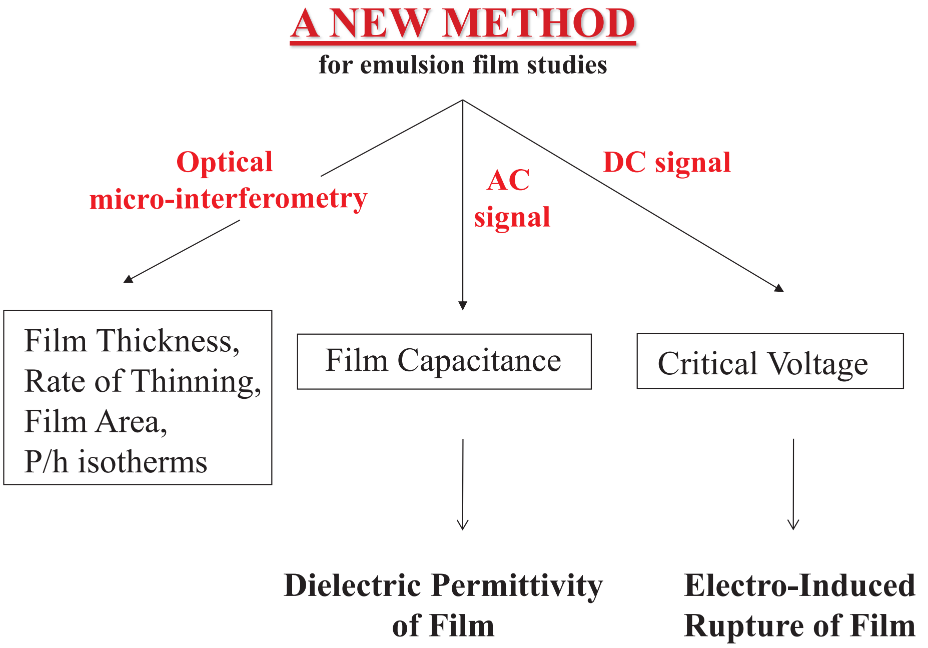

Figure 5.2.1. Parameters that can be obtained by the new method

A schematic of the new version of TLF-PBT to run optical and electrical measurements on single water in oil emulsion film is shown in Figure 5.2.2. The porous plate measuring cell (presented separately in Fig.5.2.4) was placed in a thermostating device, resting on a X-Y transverse stage and mounted on top of an inverted Axiovert 100 reflected light microscope (Carl Zeiss). The film was viewed on a monitor (Sony, PVM-14N2A,) via a CCD video camera (Hitachi, VK-C370,) and images of the film were recorded on a digital video (Sony, DSR-25). Video microscaler (FOR.A Company, IV-550) with resolution ± 1 μm was connected to the monitor to enable film diameter control with high precision. The capillary pressure was controlled by adjusting the height of the solution inside the capillary tube using a manually operated micrometer syringe (Gilmont Instruments). The film thickness was determined by the microinterferometric method of Scheludko and Exerowa using monochromatic filter ($\lambda$= 546 nm). The incident light was directed through a pin-hole or iris diaphragm creating a ~10 μm diameter spot focused onto the film. The reflected light passed through a second pin-hole diaphragm located just prior to the photodiode. The intensity of reflected light was measured with a highly sensitive low-light, low-noise Si-photodiode (Hamamatsu Corporation) and recorded using a strip chart.

VoltaLab 80 (Radiometer Analytical PGZ 402 with VoltaMaster 4 software version 5.6) was used to apply electrical polarization and to measure electrical properties of the film. A resistor of 20 MΩ was connected parallel to the measuring cell. The VoltaLab, operating within frequency range of 1mHz to 100 kHz, was controlled by a computer.

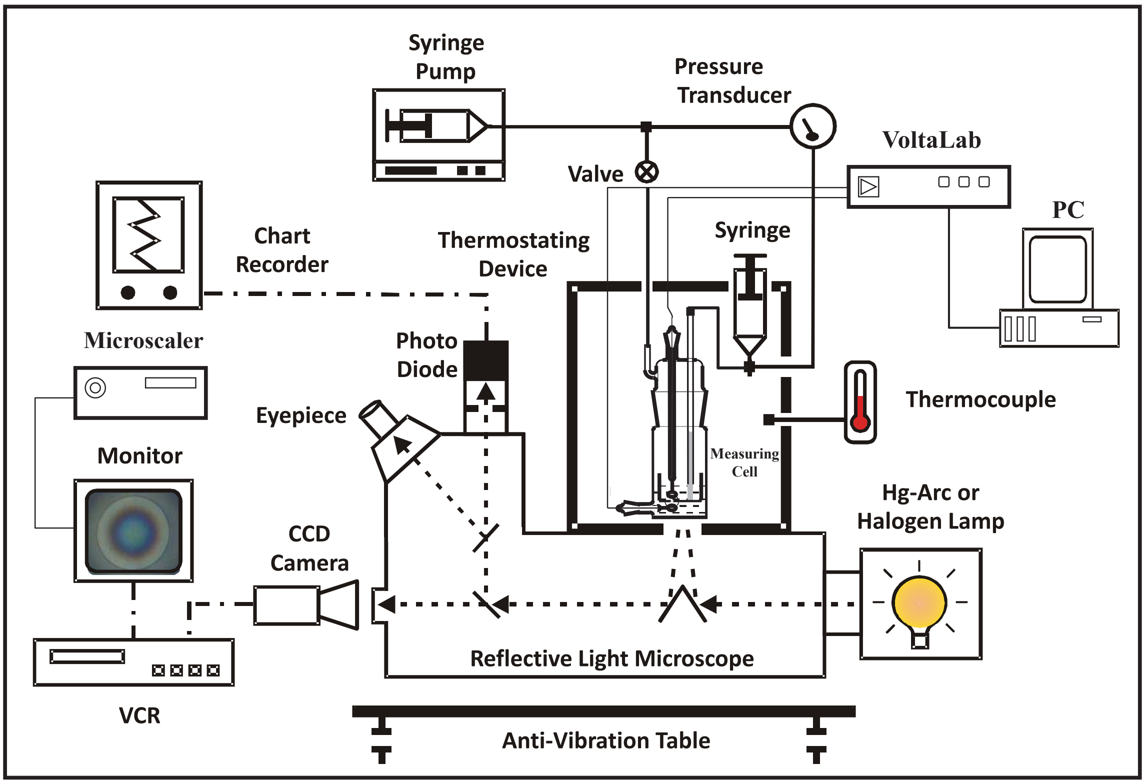

Figure 5.2.2. Upgraded TLF-PBT for optical and electrical measurements

Picture 5.2.3. The whole set-up of the thin liquid film apparatus

The core of the adapted TLB-PBL technique to study water-in-oil emulsion films is the new measuring cell, shown in Figure 5.2.4. There are two essential parts to this measuring cell: a lower part consisting of a glass cylinder with an optically flat bottom allowing the film to be viewed from below with a reflected light microscope and serving as a reservoir of the external aqueous phase. The upper part, designed so as to close the measuring cell, consists of a glass cup with a porous plate (forming the bottom of the cup) to hold the film, a capillary tube to provide the oil phase. A hole (0.75 mm diameter) to support the film was drilled into the porous glass plate. A magnification of the porous plate, film, meniscus and the pair of platinum electrodes is shown separately. The glass cup, i.e., the upper part of the cell, was immersed into the aqueous electrolyte solution contained in the reservoir forming the lower part of the measuring cell. When assembled the cell provided for the oil film to separate two electrically isolated aqueous phases: one inside the film holder cup and the other in the external reservoir. The two platinum electrodes were used to apply electrical signals across the oil film. A Faraday cage surrounded the measuring cell.

The porous plate was made hydrophobic by soaking it with solution of 20% chlorotrimenthylsilane (purity 98%, Acros) in cyclohexene (reagent grade, Fisher Scientific) for 24 hours and afterwards with 50% bitumen solution in toluene for 72 hours. Anhydrous ethyl alcohol (reagent grade, Fisher Scientific) and toluene were used for a glass cleaning procedure.

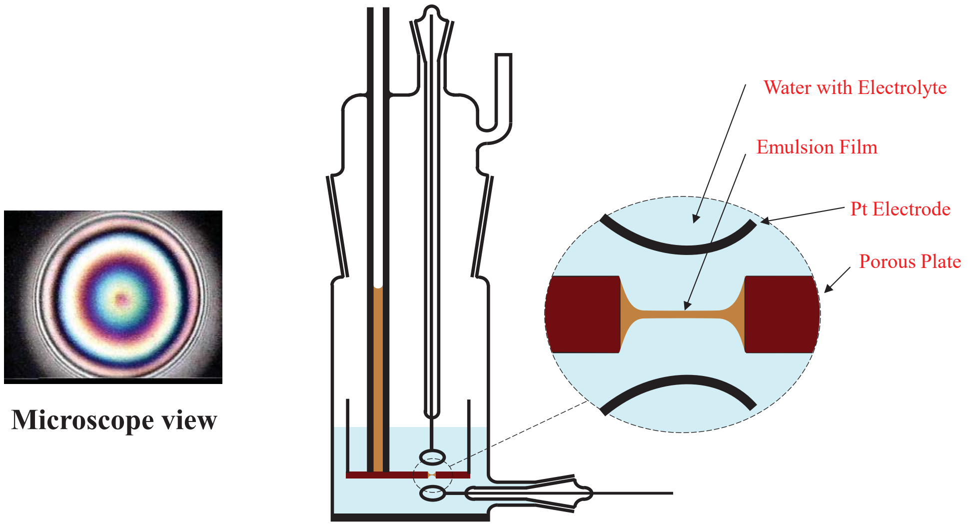

**Microscope view**

Figure 5.2.4. A modified Scheludko-Exerowa cell for electro-optical studies of emulsion films

## 5.3 Materials

In the thesis we studied both films, stabilized by model surfactants as well as formed from real complex solutions of bitumen and asphaltenes. The following systems were investigated:

- Abil diluted in decane (model system)
- Lecithin diluted in toluene (model system)
- Asphaltenes diluted in toluene (semi-real system)
- Bitumen diluted in toluene, heptane and heptol (real system)

**Synthetic surfactant Abil** is well known for its ability to stabilize emulsions and represents a comb-graft copolymer with a poly(siloxane) backbone and poly(ethylene oxide)/poly (propylene oxide) and C16 grafts (Abil EM-90) with a total number-average molecular weight of 62,000. Neither the molecular weights of the various groups or the distribution is known.

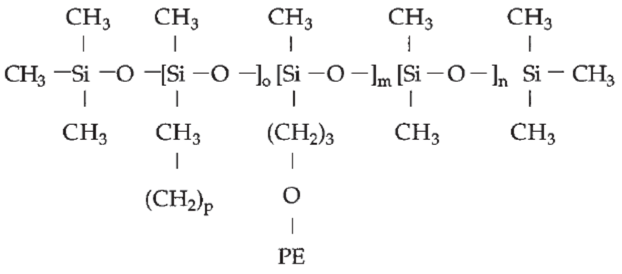

$$CH_3-\overset{CH_3}{\underset{CH_3}{Si}}-O-[\overset{CH_3}{\underset{\underset{(CH_2)_p}{CH_3}}{Si}}-O-]_o[\overset{CH_3}{\underset{\underset{\underset{PE}{O}}{(CH_2)_3}}{Si}}-O-]_m[\overset{CH_3}{\underset{CH_3}{Si}}-O-]_n\overset{CH_3}{\underset{CH_3}{Si}}-CH_3$$

$$PE = (-C_2H_4O)_x(-C_3H_6O)_y-H$$

**Lecithin** from egg yolk is another surfactant that is popular for its stabilizing properties and is a low-molecular weight (ca.800 Da) mixture of zwitterionic phospholipids containing two fatty acid chains.

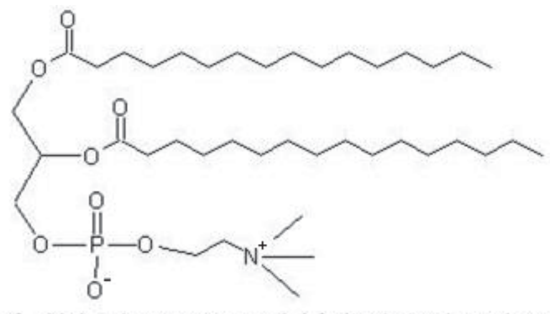

*Scheme 2. Molecular structure of 1,2-dipalmitoyl-sn-glycero-3-Phosphatidylcholine*

# Chapter 6. Concentration effects on critical voltage

The very first question that we had to answer was: can critical voltage, $V_{cr}$, be introduced as a film stability parameter? If so, it is to be expected that with increase of surfactant concentration the stability of films under the action of external voltage should increase. Therefore, our first task was to examine if critical voltage parameter will be sensitive enough and will show any signs of increase with concentration.

### 6.1.1 Effect of concentration of bitumen-diluted-in-toluene

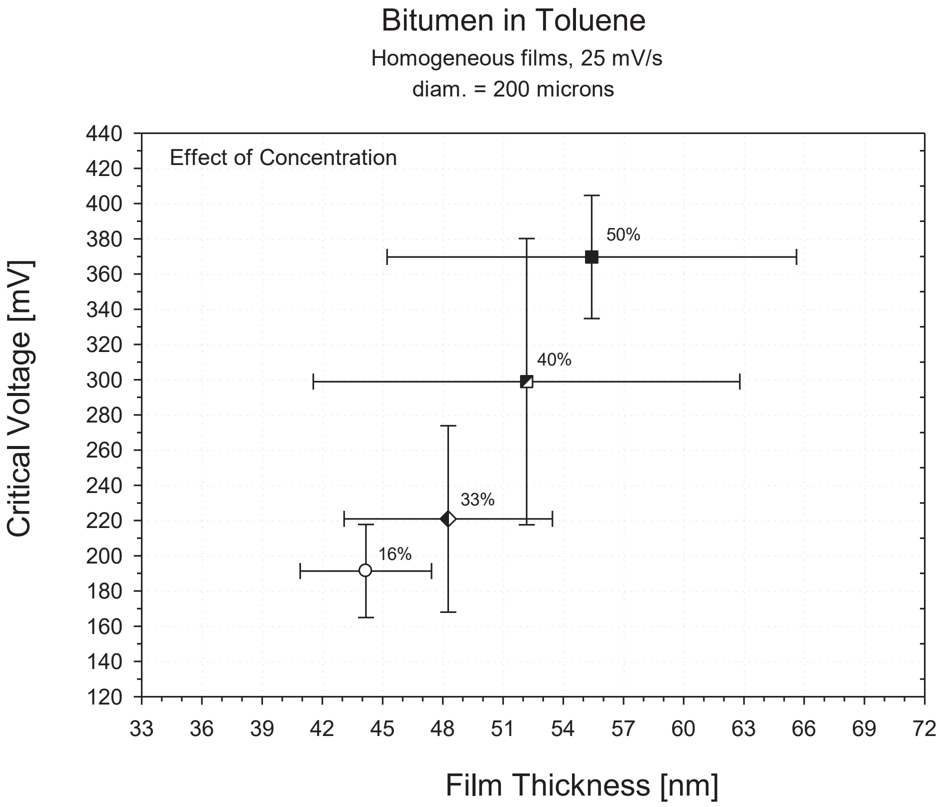

Figure 6.1.1. Effect of concentration of bitumen-diluted-in toluene on critical voltage

Figure 6.1.1 shows that increase of bitumen content that is being diluted in toluene leads to higher voltages of rupture. All films have constant diameter of 200 μm and voltage ramps (25 mV/s) are applied on equilibrium films having respective homogeneous thicknesses. The concentration range studied was 16 ÷ 50%. It is also evident that increase of concentration is followed by formation of thicker equilibrium films.

Comparison between the mean values of electric field strengths at various concentrations are shown in the table below.

| Conc. [%] | E [mV/nm] |
|---|---|
| 16 | 4.3 |
| 33 | 4.6 |
| 40 | 5.8 |
| 50 | 6.7 |

Table 6.1.1. Effect of concentration of bitumen-diluted-in toluene on critical field strength

Thus, besides the critical voltages, the parameter field strength also suggests increase of stability with concentration.

### 6.1.2 Effect of concentration of bitumen-diluted-in-heptane

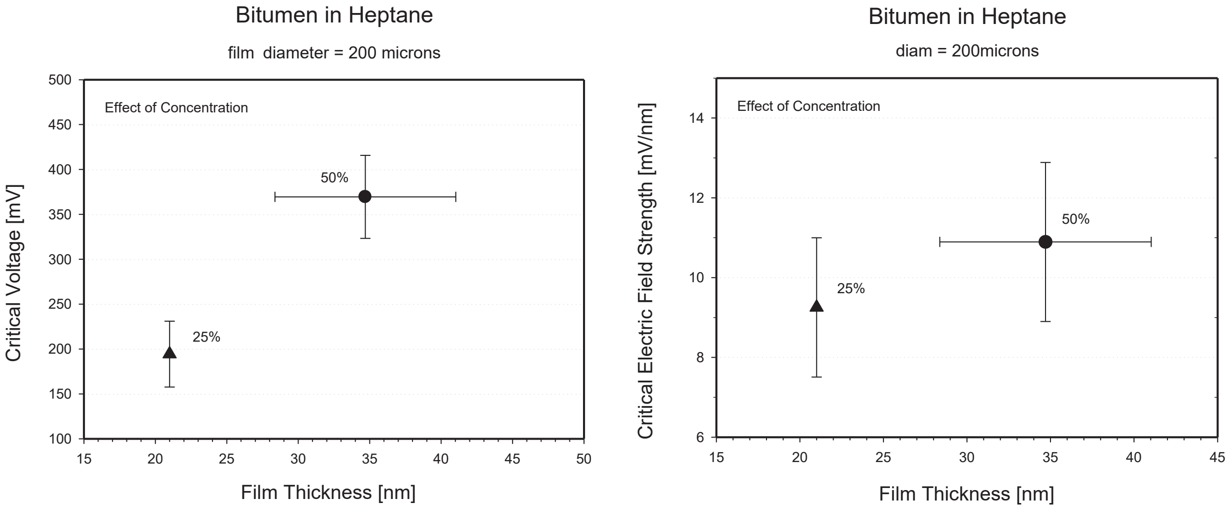

Figure 6.1.2. Effect of concentration of bitumen-diluted-in heptane on A) critical voltage and B) critical electric field strength

### 6.1.3 Effect of concentration of asphaltenes-diluted-in-toluene

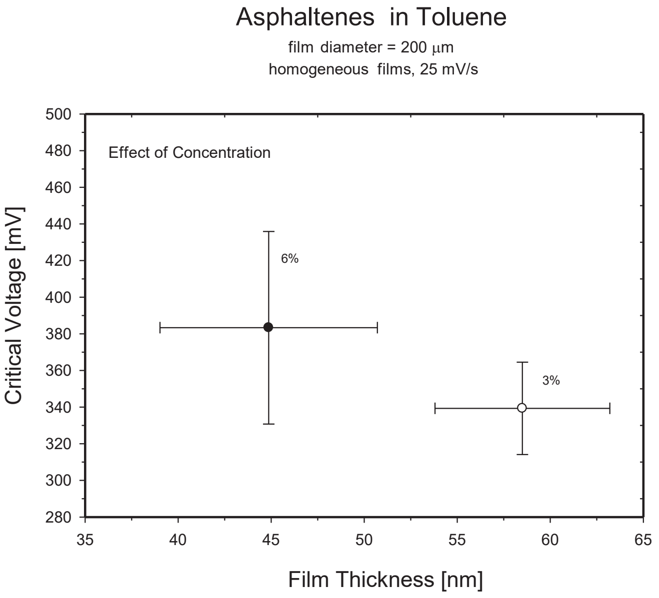

Figure 6.1.3. Effect of concentration of asphaltenes-diluted-in-toluene on critical voltage

As in the case of bitumen films, all asphaltenic films were 200 μm in diameter and were homogeneous in equilibrium thickness. Obtained mean critical voltage values and their spread demonstrate that increase of asphaltene content leads to formation of more stable films. Comparison between the electric field strengths that films at both concentrations can withstand also suggests that films at higher concentrations are more stable. Mean values of the electric field strength for 6% concentration is 8.5 mV/nm (383/45) vs. 5.9 mV/nm (340/58) for 3% films.

### 6.1.4 Effect of concentration of lecithin-diluted-in-toluene

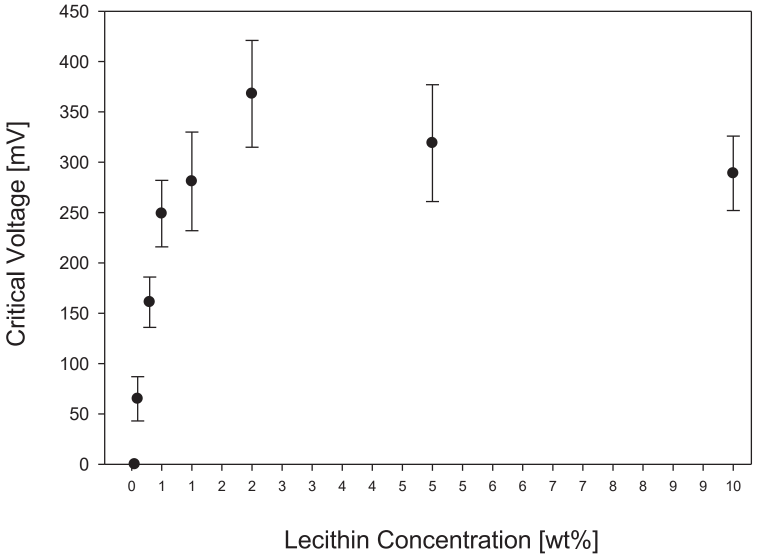

Figure 6.1.4. Effect of concentration of lecithin-diluted-in-toluene on critical voltage (film diam.=200 μm, 25 mV/s ramps)

Figure 6.1.4 shows increase of stability with concentration followed by appearance of some sort of plateau. In these model experiments, initially the concentration was changed with very narrow increments. Despite of this the obtained sensitivity of critical voltages was impressive, the values rose from 50 mV to some 400 mV with much less overlaping of scatered data. In this respect there is much pronounced difference compared to complex bitumen and asphaltenic systems. Thus, the results clearly demonstrate the necessity of studying chemically well defined model systems and further confirm the applicability of the method.

## 6.2 Effect of the type of bitumen

On Figure 6.2 it is shown the comparative study between heavy and light bitumen samples. Equilibrium films from heavy bitumen are much thinner than corresponding light bitumen films.

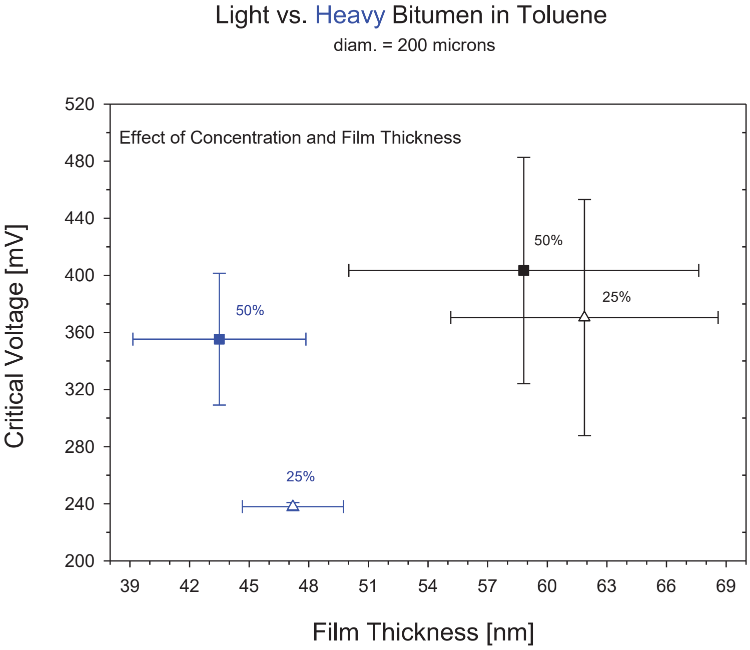

Figure 6.2. Effect of concentration of light bitumen (symbols on the right side) and heavy bitumen (on the left side)-diluted-in-toluene on critical voltage

| Conc. [%] | E [mV/nm] |
|---|---|
| 25 (heavy) | 5.1 |
| 25 (light) | 6 |
| 50 (heavy) | 8.2 |
| 50 (light) | 6.8 |

Table 6.2. Effect of concentration of light and heavy bitumen-diluted-in-toluene on critical field strengths

For the light films, neither critical voltage values nor field strengths suggest significant effect of concentration on stability, while this is not the case for the heavy films. Also, at the first quick glance on critical voltages one can conclude that heavy bitumen films are less stable. However, the field strength parameter again becomes useful since it demonstrates that heavy bitumen films are more stable than light bitumen films at 50%, i.e. relatively similar critical voltages should be applied on much thinner "heavy" films. At this moment we may only speculate that one possible reason, amongst others, is that thinner films become more structurized/ordered and this could contribute to their strength. At lower concentration of 25%, relatively close values of field strengths for the two types of bitumen show rather similar stabilities. However, obtained critical voltages differ significantly. We may conclude that in most of the studied cases the field strength parameter confirms the inferences from critical voltage values, but in some cases it may reverse the stability trends.

Finally, the following main experimental findings could be summarized so far:

- From the available experimental material it is evident that the two stability parameters are sensitive enough to concentration changes, to the type of surfactant, and to the type of the organic solvent.
- For the case of bitumen films diluted in toluene, equilibrium thickness increased with increase of concentration. Within the concentration range 16 ÷ 50%, mean values of critical voltages rose from 190 mV up to 370 mV, while mean critical electric fields increased from 4.3 mV/nm up to 6.7 mV/nm.
- Equilbrium bitumen films diluted in heptane also get thicker with change of concentration from 25% up to 50%. These films show similar increase of critical voltages, however their mean critical field strengths are much higher (9.3 mV/nm and 11 mV/nm) than respective toluene-diluted films due to their overall smaller thicknesses.
- Unlike bitumen films, asphaltenic films in toluene do not show increase of equilibrium thickness with concentration, but on a contrary. Increase of asphaltenic content from 3% up to 6% leads to decrease of mean equilibrium thickness from 58 nm down to 45 nm. Obtained mean critical voltages (340 mV vs 383 mV), their spread along with mean critical fields (5.9 mV/nm vs 8.5 mV/nm) show moderate increase of stability with concentration.
- Comparison of critical voltages between toluene-diluted bitumen and asphaltenic films at around 45 nm thickness (mean value) shows that asphaltenic films are much more stable despite their significantly lower concentration.
- Model lecithnin-stabilized films in toluene demonstrate that within the very narrow concentration range 0.2% ÷ 2%, the obtained increase of critical voltages was impressive (50 mV÷400 mV) with much less overlaping of scatered data. In this respect there is much pronounced difference in sensitivity of model lecithin films compared to complex bitumen and asphaltenic systems.

# Chapter 7. Electric field-induced film dynamics

In this section, based on model Abil system, a new type of isotherm is introduced, namely DC voltage-thickness isotherm and the corresponding electric field-thickness isotherm.

## 7.1 DC Voltage-Thickness isotherms for Abil films

In this experimental design, film thickness is monitored constantly during the entire application of voltage ramps up until the rupture. Such approach allowed the construction of a voltage-thickness isotherms. The obtained results present evident proof of compressive action of applied external DC field and provide details on the changes that film undergoes.

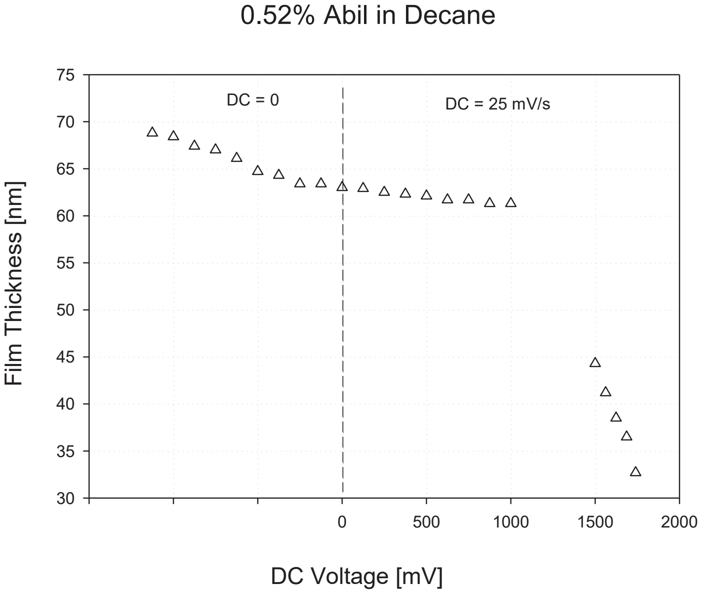

Figure 7.1. Voltage-thickness isotherm for 0.52% Abil-in-decane film, diameter =500 μm

Non-equilibrium film drains very slow without application of DC voltage and eventually reaches the equilibrium thickness of 63 nm. At this stage the external voltage is applied in form of ramps with rate 25 mV/s. Initially, the increase of voltage is small and up to 1000 mV the film thickness remains almost the same, i.e. only a slight decrease of 2 nm is observed. Further increase of voltage leads to remarkable reduction in film thickness and loss of stability. Within the range 1000-1500 mV many white dots (and probably dimples) appear, which makes quite impossible measurement of thicknesses. At a given voltage of 1015 mV, film thickness starts to decrease sharply. We decided to name this voltage a “threshold” voltage. Finally film ruptures at critical voltage of 1740 mV and rupture thickness of 32.7 nm.

### 7.1.1. Reproducibility of voltage-thickness isotherms

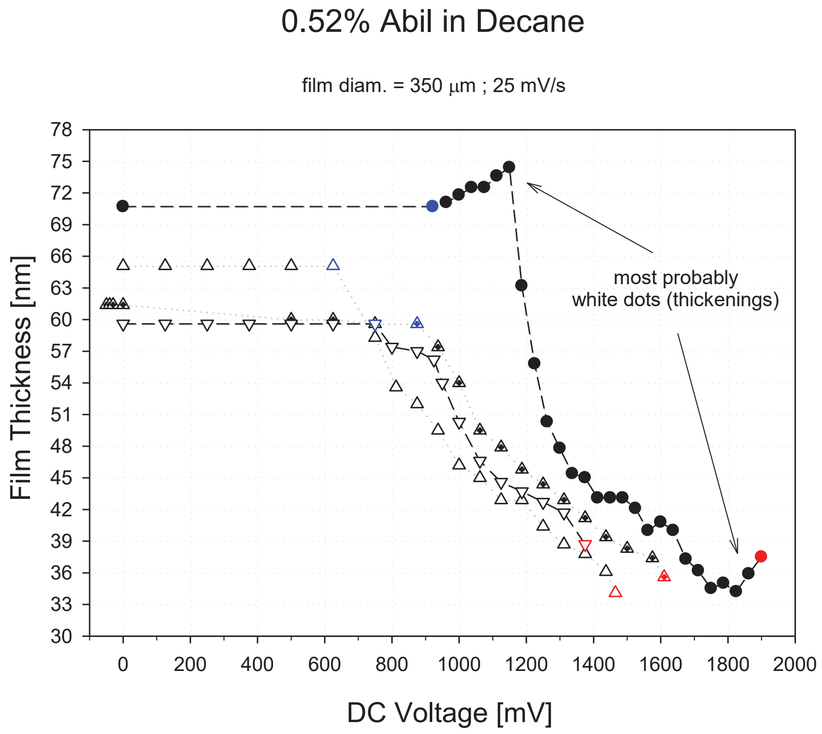

Figure 7.1.1. Reproducibility of voltage-thickness isotherm for 0.52% Abil-in-decane films, diameter =350 µm (red and blue symbols denote rupture and threshold values, resp.)

The main goal here was to investigate the reproducibility of voltage-induced film dynamics. In all cases, immediately after DC application white dots appeared within the films and after a while these thick ’’islands’’ dissapeared. It should be mentioned that during the formation of this ‘‘network‘‘ of white dots the film area between dots gets darker, hence thinner. Due to the size of the used optic blenda, the exact thickness in these places was difficult to be measured. The appearance of these dots might suggest that squeezed liquid from the film is collected within the observed white thickenings. Furthermore, formation of these thickenings varies quite in time amongst the experiments and can take place either before the threshold voltage, or after it, or sometimes do not appear visibly. However, they always show up right after the initial voltage stress is applied. Generally speaking, curves on the figure demonstrate reasonable reproducibility considering the stochastic nature of appearance of threshold instability and the final rupture.

## 7.2 Electric field strength – thickness isotherms

Next figure represents the same experiment, but the results were plotted in coordinates of electric field strength vs. film thickness. A quick glance shows the reproducibility having the curves stacked together. Threshold field strengths, at which films start loosing their stability is within the range 10-15 mV/nm.

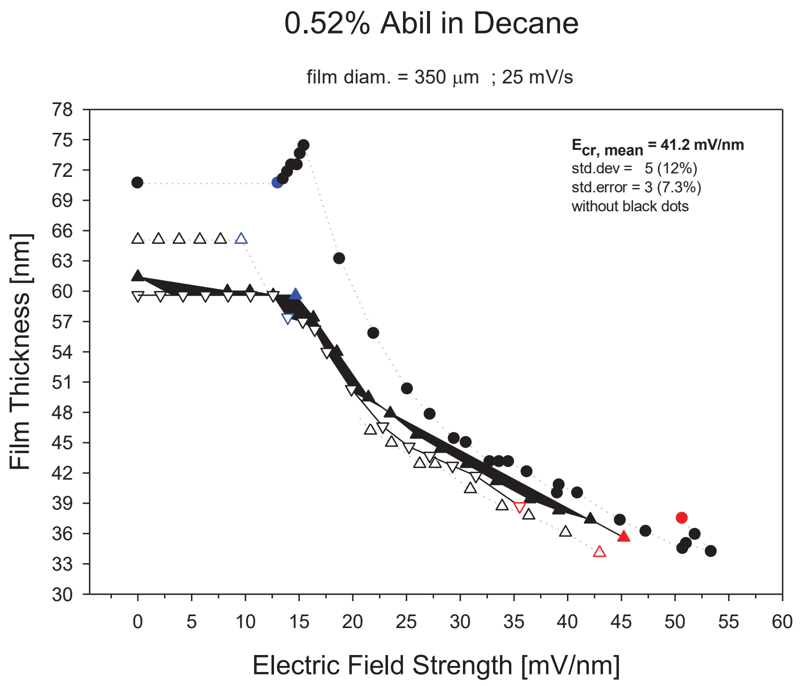

Figure 7.2.1. Reproducibility of electric field strength-thickness isotherms for 0.52% Abil-in-decane films, diameter =350 μm (red and blue symbols denote rupture and threshold values, resp.)

## 7.3 Voltage-thickness isotherms at various film sizes

Next set of results illustrates films that are within broader range of diameters, 200 – 750 μm. For the largest film (black circles) thickness was measured in the thinnest part since film shows significant thickness profile. For the rest of the films thickness was measured in the center.

First thing to be mentioned is the lack of dependence of thickness-voltage isotherms with film size. To some extent this indifference on the size is due to the fact that appearance of the threshold (onset of instability) doesn't seem to depend on the dimensions of the films. And it is apparent that threshold occurrence largely conditions the voltage-thickness course of the curves. Generally speaking, it could be noted that once instability starts, the slopes of the curves (speed of the forced thinning) seem to be pretty similar and visibly somewhat parallel to each other. Broadly speaking, higher the threshold values higher the critical values appear to be.

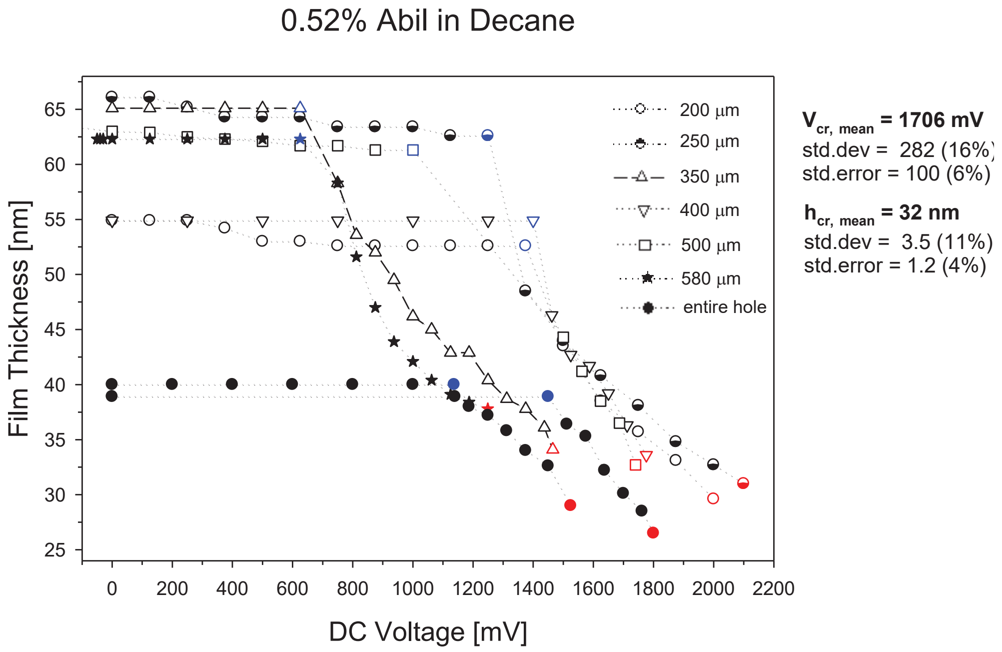

Figure 7.3.1. Voltage-thickness isotherms for 0.52% Abil-in-decane films, diameters = 200-750 µm, 25 mV/s (red and blue symbols denote rupture and threshold values, resp.)

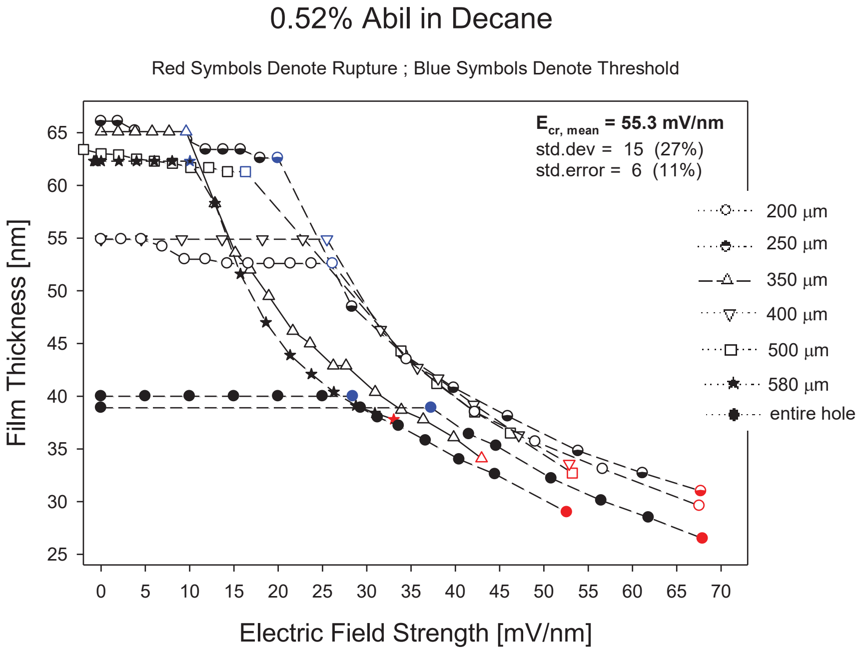

Figure 7.3.2. Electric field strength-thickness isotherms for 0.52% Abil-in-decane films, diameters = 200-750 µm, 25 mV/s (red and blue symbols denote rupture and threshold values, resp.)

## 7.4 Voltage-thickness isotherms at different rates of voltage ramps

Majority of the experiments were conducted at voltage ramps with speed of 25 mV/s. On the graphs below are illustrated just some of the exemplary results within the ramps range 5÷150 mV/s. All values fell within the scattering of the results, more importantly one couldn’t find some trend on the speed of ramps.

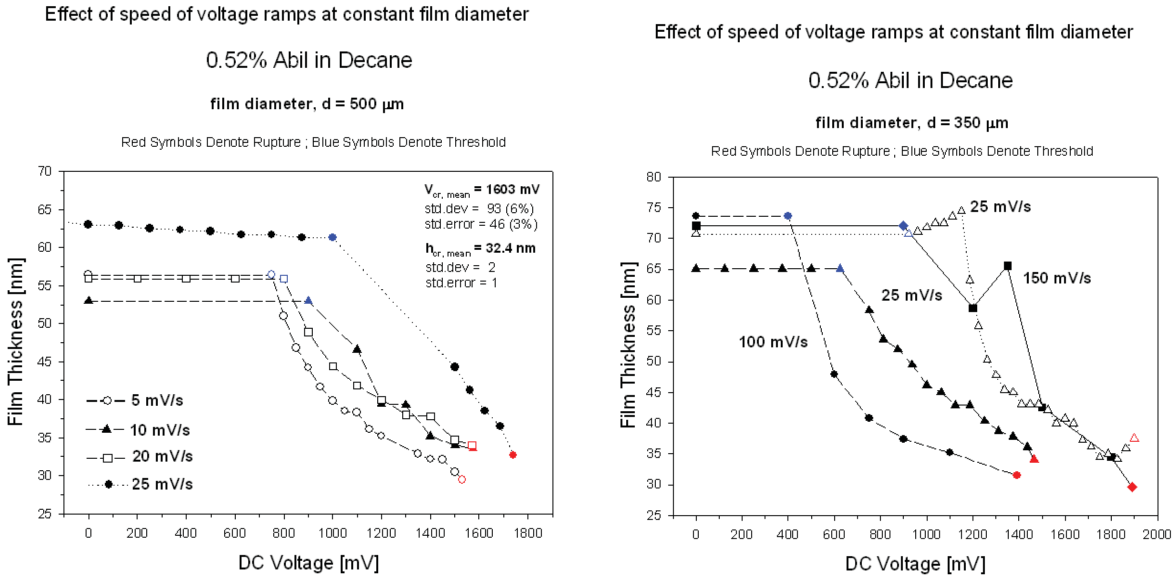

Figure 7.4.1. Voltage-thickness isotherms for 0.52% Abil-in-decane films at different film diameters and voltage ramps. a) 500 µm, b) 350 µm

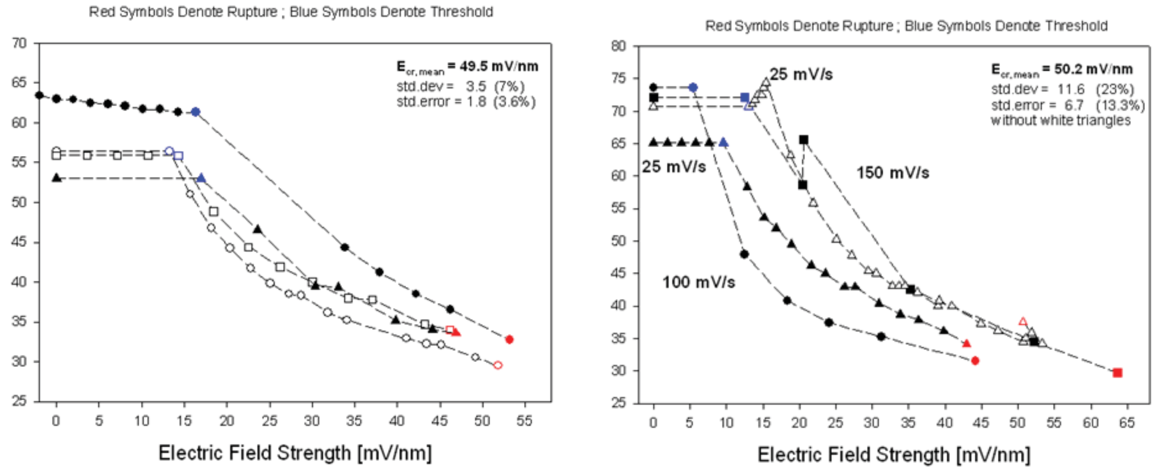

Figure 7.4.2. Electric field strength-thickness isotherms for 0.52% Abil-in-decane films at different film diameters and voltage ramps. a) 500 µm, b) 350 µm

## 7.5 Effect of capillary (mechanical) pressure on voltage-thickness isotherms

Next approach included imposition of higher mechanical pressures on electrically stressed films. These pressures were kept constant during the corresponding experiments. In this manner, the goal was to examine if electrical instability was respondent to extra pressing from the external environment. Figure 7.5 shows the results for Abil-stabilized decane films at three different applied capillary pressures.

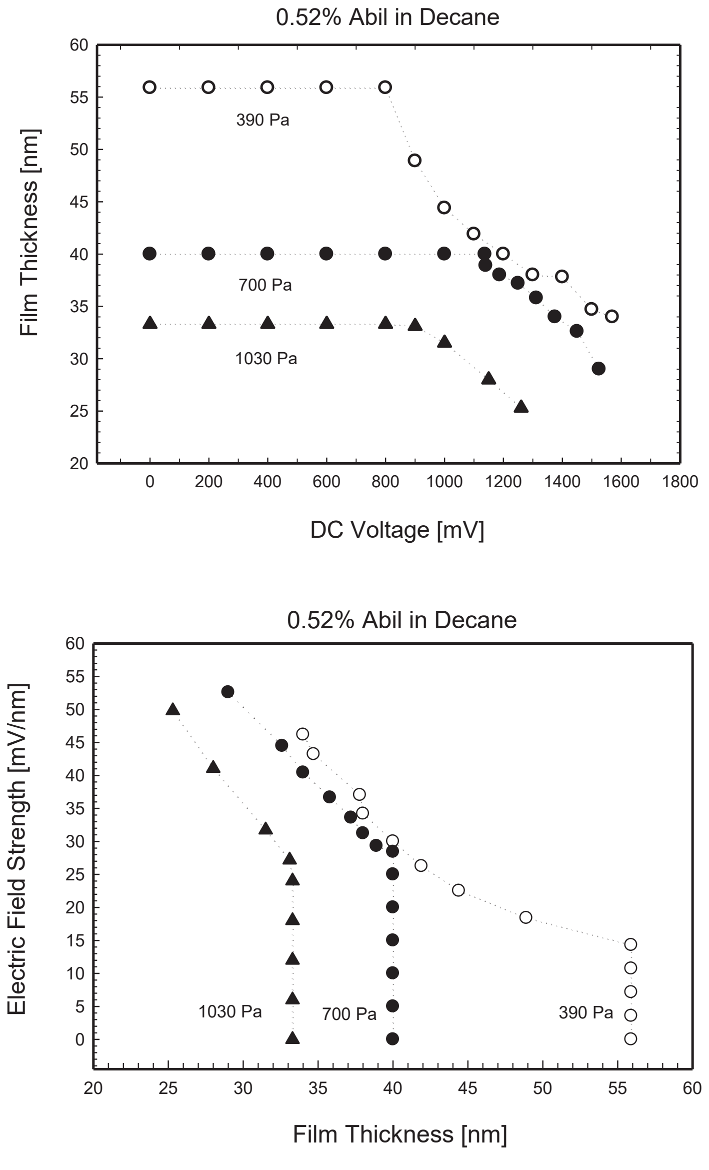

Figure 7.5. (top) Effect of DC ramps (25 mV/s) on film thickness at different applied pressures; (bottom) Build-up of electric field strengths at different pressures.

Increase of applied capillary pressure (without voltage) leads expectedly to decrease of equilibrium film thickness. This highest pressure is just on a brink of the rupturing pressure for the films without DC. Furthermore, at the highest capillary pressure the thickness of rupture fell down to about 25 nm, a value not seen for homogeneous films at low pressures. Next, again at the highest pressure, the critical voltage was diminished to less than 1300 mV. This is somewhat reduction of this value compared to the range 1400÷2100 mV that corresponds to low formation pressures. However, the balance between decreased rupture thickness and decreased critical voltage leads to formation of similar critical electric strengths.

### 7.6 Effect of voltage application on mechanical pressure-thickness isotherms

Another experimental approach that the proposed method allows is to work in the mode of gradual increase of the capillary pressure, while maintaining constant DC voltage. This enables the introduction of another parameter describing film stability, namely critical mechanical pressure of rupture at certain DC voltage. This parameter apparently contains the combined effect of mechanical and electrical stresses on stability. Thus, construction of such isotherm provides opportunity for investigation of the effect of electrical polarization on interfacial forces.

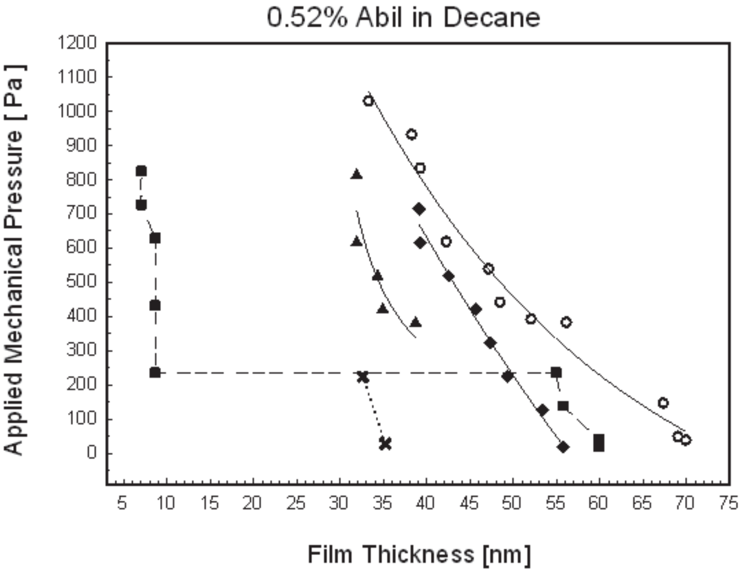

Figure 7.6. Measured isotherms capillary pressure-thickness at different applied DC voltages: 0 mV (circles); 500 mV (squares); 1000 mV (diamonds); 1350 mV (triangles); 1500 mV (x). The isotherm at 500 mV undergoes transition to very thin black film and, eventually, no rupture.

The film at 500 mV was not ruptured due to the transition to very thin black film. The isotherm of this film (after the sudden jump to much thinner thicknesses) resembles quite well the isotherms of sterically stabilized films. It should be mentoned that such a transition occurred in rare occasions amongst many experiments.

At no voltage applied, the critical pressure was 1025 Pa. The isotherm at 1000 mV shows that the voltage action leads to lower value of critical pressure, i.e. 720 Pa. Further, at 1500 mV we could measure only two points due to high polarization of film interfaces and rupturing pressure was only 225 Pa. Overall trend for decrease of critical pressure with the DC field is noticeable.

From fig.7.6 it is evident also that increase of polarization shifts the isotherms towards lower equilibrium thicknesses, hence affecting the acting interfacial forces within the films. This experimental fact presents another illustration for the compressive action of DC polarization.

# Chapter 8. Experimental indications for the mechanisms of electro-induced film break-up

## 8.1 Rupture of thick bitumen films occurs via formation of black spots

Figure 8.1 shows images of the equilibrium film (no voltage is applied) and during the voltage probing. At given DC potential, black thin spots start to appear at the film periphery. With further increase of the potential these spots grow in size and become more pronounced. At certain critical potential film ruptures, presumably in the thinnest place of periphery. Thus, formation of black spots at the film periphery with the expulsion of drained material to the meniscus gives experimental clues for the possible mechanism of break-up of thick grey films.

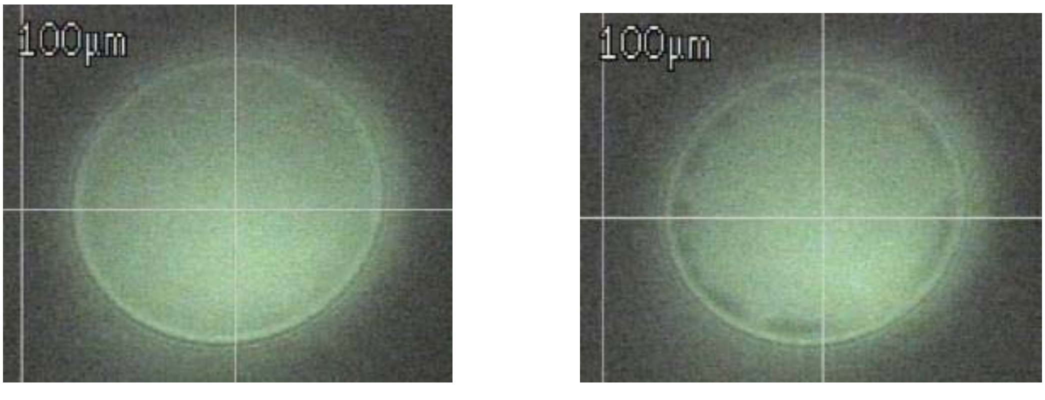

Voltage = 0

Applied voltage

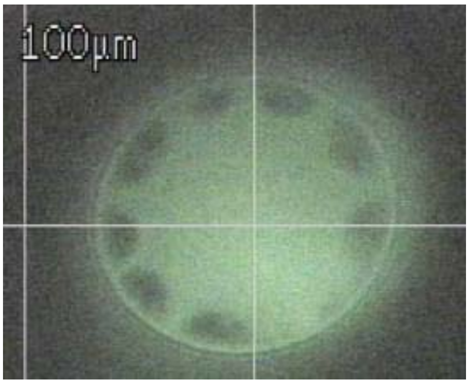

Critical voltage

Figure 8.1. Photomicrograph images during the application of DC potential on 33% toluene-diluted bitumen films

## 8.2 Rupture of thin black bitumen films occurs via formation of white spots

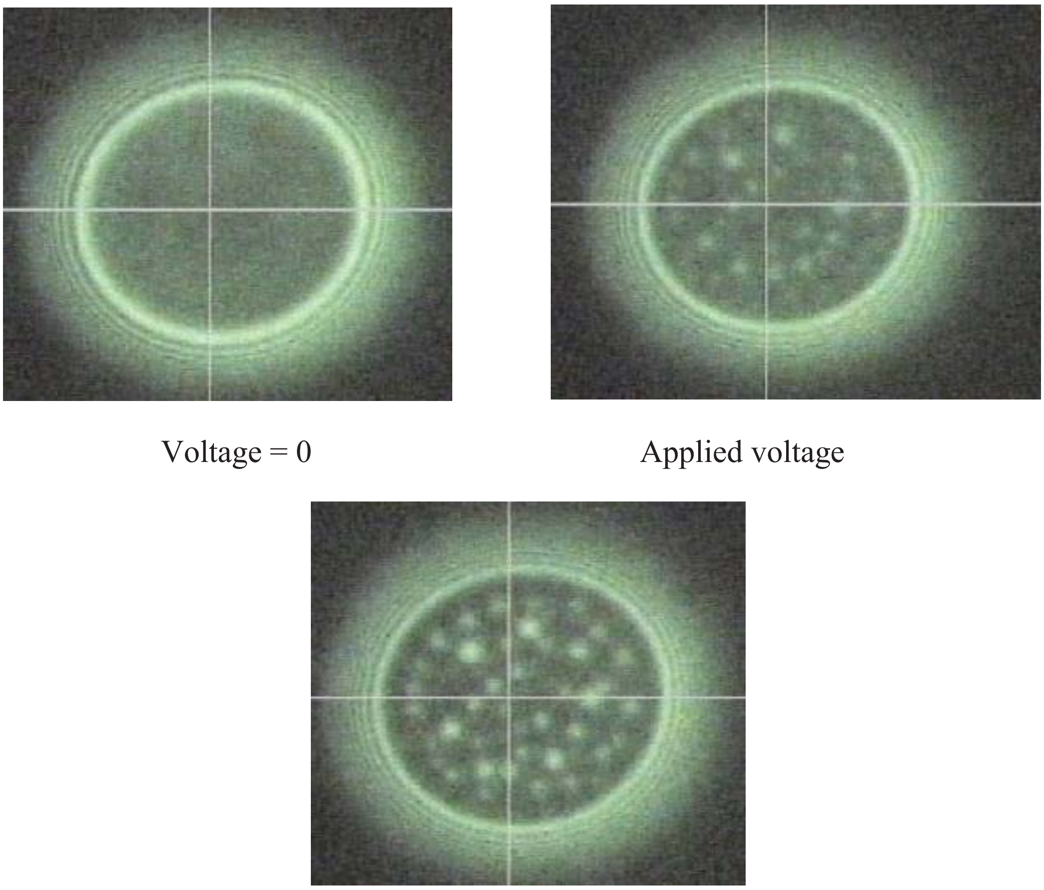

Voltage = 0

Applied voltage

Critical voltage

Figure 8.2. Photomicrograph images during the application of DC potential on 25% heptane-diluted bitumen films

Figure 8.2 depicts much different picture for the appearance of electro-hydrodynamic instabilities in the case of thinner black films. At a given potential, thick white spots formed within the entire film area. Further increase of potential was followed by the increase of the number of these thick islands, which become even more distinctive. It is to be assumed that with the enhance of the compressive action of DC voltage, film undergoes further thinning so that the squeezed material is being collected in the growing local thickenings, while the background of the film darkens further. Eventually film ruptures somewhere between these spots, in the thinnest place of the film.

### 8.3 Electrical conductivity measurements

In Figures 8.3.3 and 8.3.4 the results of DC conductance behavior are displayed for model systems of lecithin-stabilized toluene films and Abil-stabilized decane films. When the film is intact at low potentials, the conductance of the system will be extremely low owing to the highly capacitive nature of the predominantly dielectric oil film. The current is very low (in nA range) and linearly increases with the potential. During this stage, the two interfaces of the film, which acts as a capacitor, acquire a charge.

Once the potential reaches the critical value, the film ruptures, the stored charge is released and dissipated, and rapidly migrates toward the electrodes. Hence, the conductance increases sharply (goes in μA range) as the merging water phases establish an electrically conducting pathway.

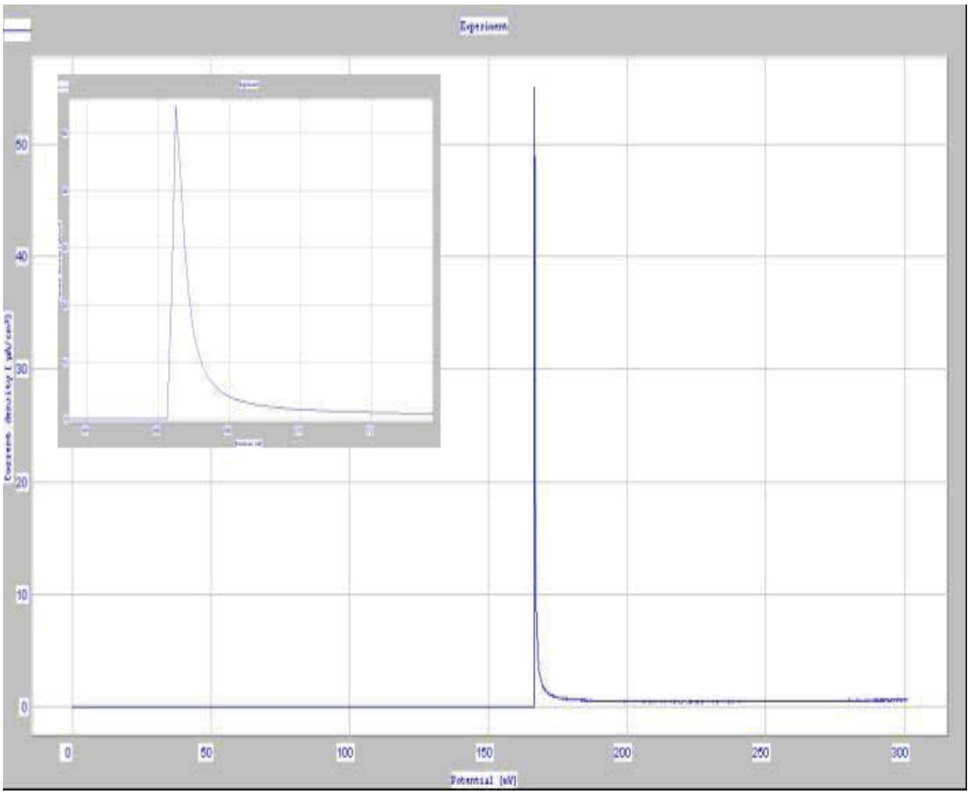

Figure 8.3.3. Current density vs. applied potential for lecithin stabilized (0.5%) films in toluene. Inset displays the zoomed current spark. No current leakage prior to film rupture.

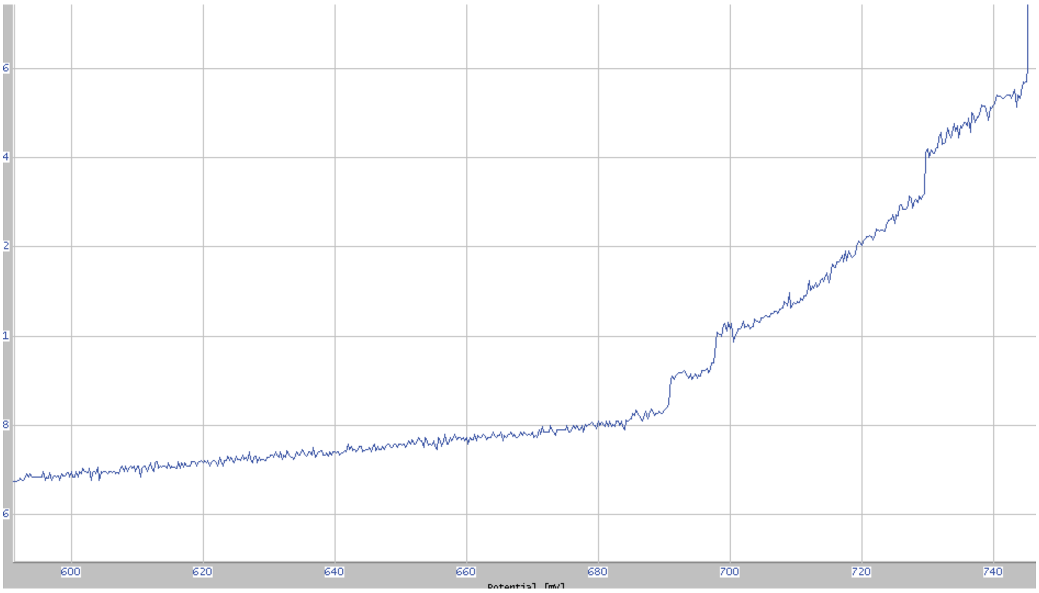

Figure 8.3.4. Current density vs. applied potential for Abil stabilized (0.52%) films in decane. Current leakage detected by the change of slope, prior to film rupture (vertical jump).

The conductance curve for the lecithin film in toluene indicates that the current passage through this film is negligible prior to the rupture of the film. The Abil film in decane, on the other hand, leaks current during the later stages of polarization and shows a substantial leakage just before breakup. The higher conductivity of the Abil film might be due to the conductivity of Abil molecules. Similar polymers with dimethyl siloxane backbone are well-known for their conductive characteristics. Other possible mechanisms of charge transfer across a film or a nonconducting medium such as electroporation or charge transfer through micelles have been postulated for such polymer stabilized films.

### 8.4 Application of DC Potential Cycles, +500/-500 mV

Figure 8.4 shows direct application of large voltages of different polarity on Abil stabilized films in decane. This approach differs from gradual imposition of voltage ramps, so that film experiences immediately the effect of high electric stress with instant formation of distinctive intsabilities.

Once the electric field was removed, the instabilities disappeared, and the films reestablished their uniform thickness at equilibrium state, ca. 60 nm. This demonstrates the reversibility of compressive-decompressive action of DC voltage.

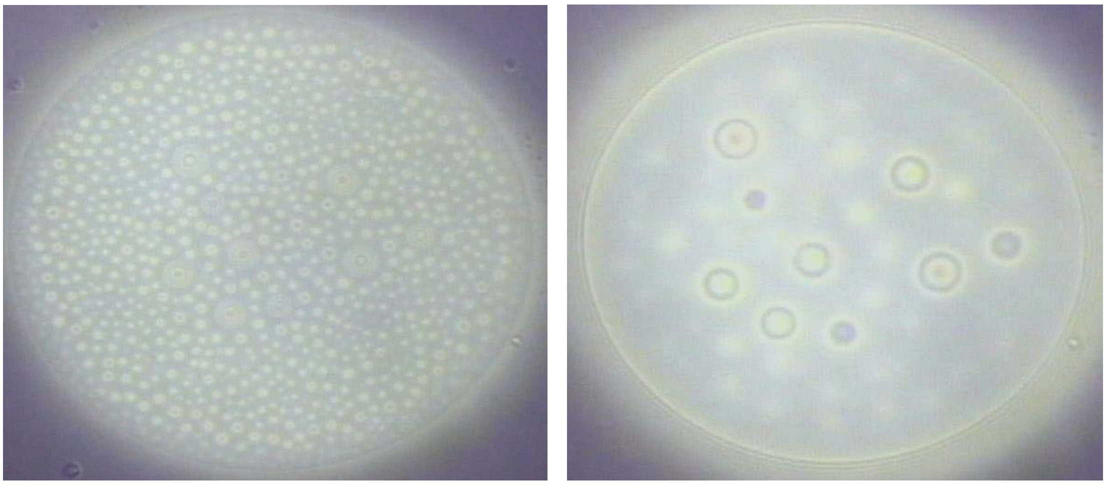

a) b)

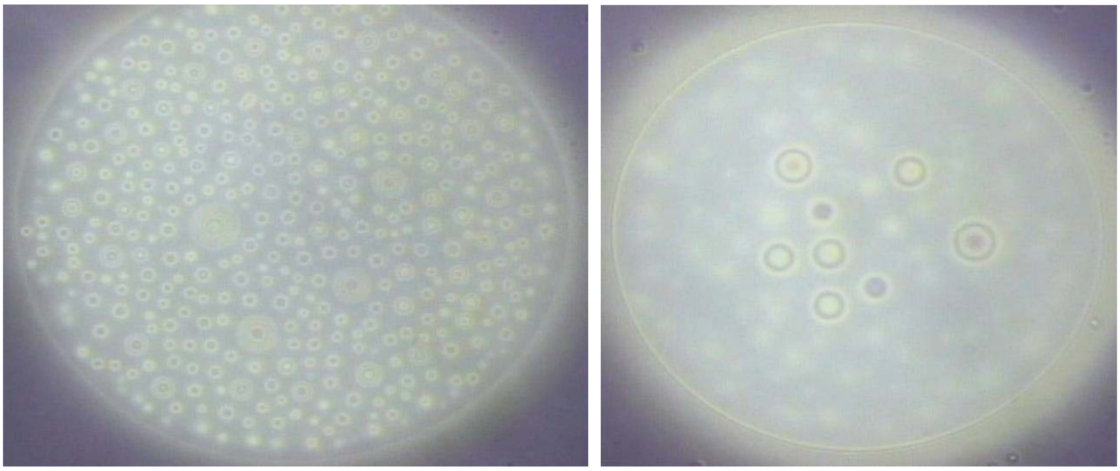

c) d)

Figure 8.4 . Application of DC cycles on 0.52% Abil films in decane. a) instant after +500 mV applied, b) +500 mV maintained, c) instant after – 500 mV applied, d) -500 mV maintained

# Chapter 9. Effect of film area on critical voltage

## 9.1 Films from heavy bitumen-diluted-in-toluene

Figure 9.1 depicts results for studied film diameters comprising the range from 50 μm up to 800 μm. Despite of the fact that there is limited number of experiments from a statistical point of view, the impression is for the lack of apparent dependence on film size. This is well seen for the case of lower concentration (33%), when all data lie within the scattering of the values for 200 μm films.

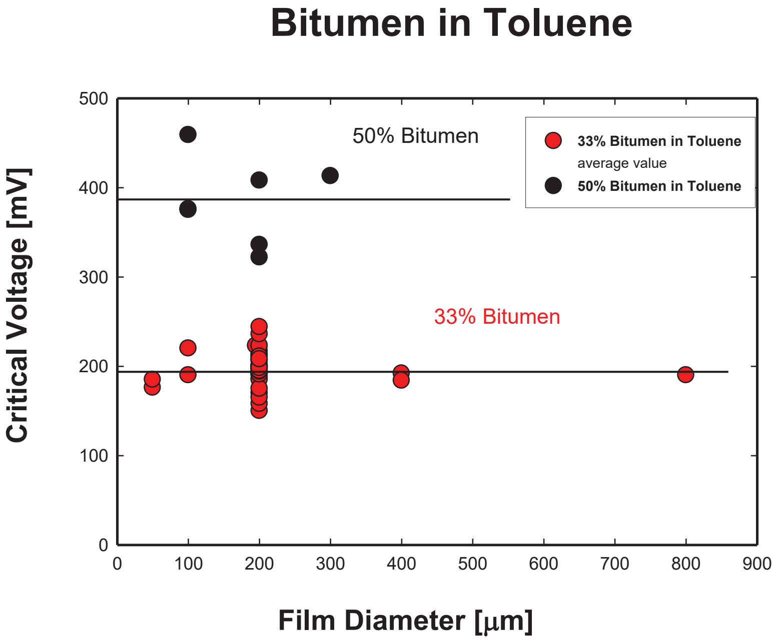

Figure 9.1. Independence of critical voltage on film diameter for films formed from heavy bitumen-diluted-in-toluene.

## 9.2 Films from light bitumen-diluted-in-toluene

Figures 9.2 show the dependence of stability of bitumen films at two concentrations, 50 and 25%. The films at high concentrations were examined within the range of film diameters 100-300 µm, while the films at low concentrations varied in diameters within the range 200-500 µm. All studied films appeared to be visibly homogenious and voltage ramps were applied on equilibrium films, which thickness is depicted on the graphs.

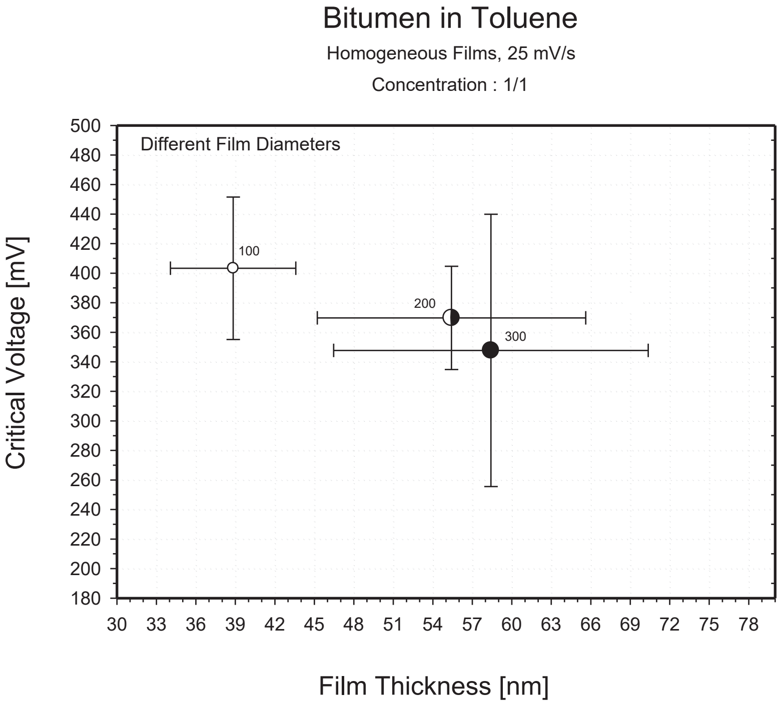

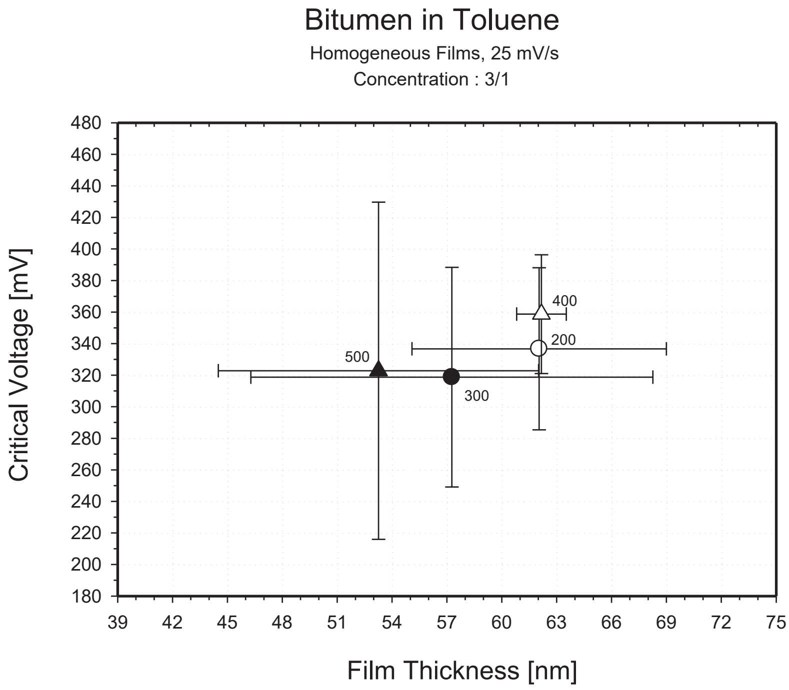

Figure 9.2. Independence of critical voltage on film diameter for films formed from light bitumen-diluted-in-toluene. (top) bitumen concentration 50%, (bottom) bitumen concentration 25%.

| **Conc. [%]** | **Film Diam. [μm]** | **E [mV/nm]** |
|---|---|---|
| 25 | 200 | 5.5 |
| 25 | 300 | 5.6 |
| 25 | 400 | 5.8 |
| 25 | 500 | 6 |
| 50 | 100 | 10.2 |
| 50 | 200 | 6.7 |
| 50 | 300 | 5.9 |

Table 9.2. Mean critical field strengths for films formed from light bitumen-diluted-in-toluene.

For low concentration films it is obvious that within the given range of film diameters, measured critical voltages (and their overlappings) as well as mean field strengths do not suggest dependence of stability on film size. For the case of high concentrations the picture looks a bit more intriguing. Between 200 and 300 μm films apparently no dependence exists in terms of mean critical voltages, though scattering for the bigger films appears much larger. Small films at 100 μm, however, appear to survive quite high electric strengths (10.2 mV/nm). This is due to a bit higher critical voltages and mainly due to their much smaller thicknesses.

### 9.3 Films from asphaltenes-diluted-in-toluene

Lastly, for the case of films stabilised by asphaltenes, a rudimentary check for the possible effect of film size on the critical voltages reveals no appearance of such dependence. It is to be noticed the wide range of diameters, 100÷700 μm, and all obtained values being comprised within the scattering of the data for the most measured films (200 μm).

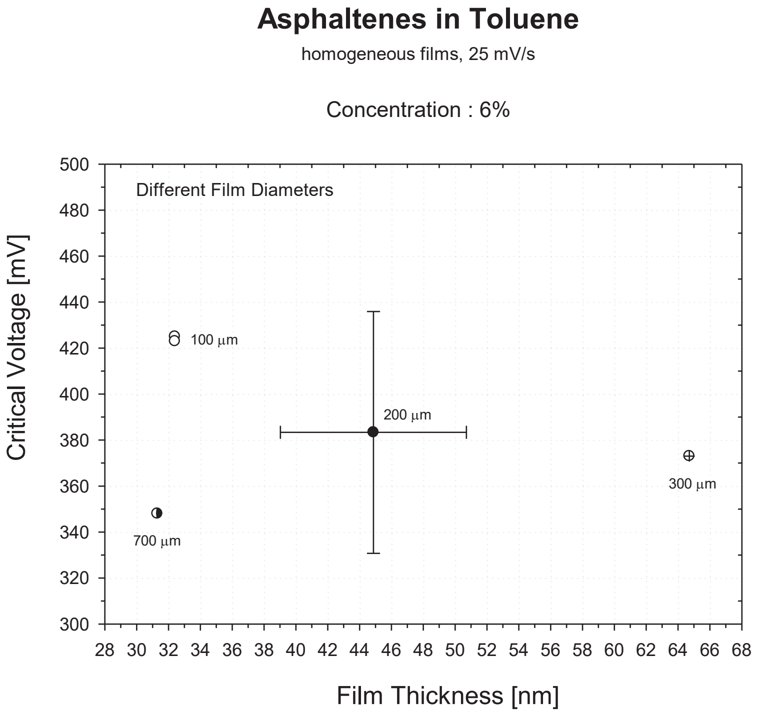

Figure 9.3. Independence of critical voltage on film area for films formed from asphaltenes-diluted-in-toluene.

### 9.4 TLF-PBT vs. Microfluid Chip. Lecithin films.

Figure 9.4.2 depicts the variation of the critical potential with lecithin bulk concentration in toluene for films, formed in the modified porous plate cell (TLF-PBT) and in the micro-fluid chip.

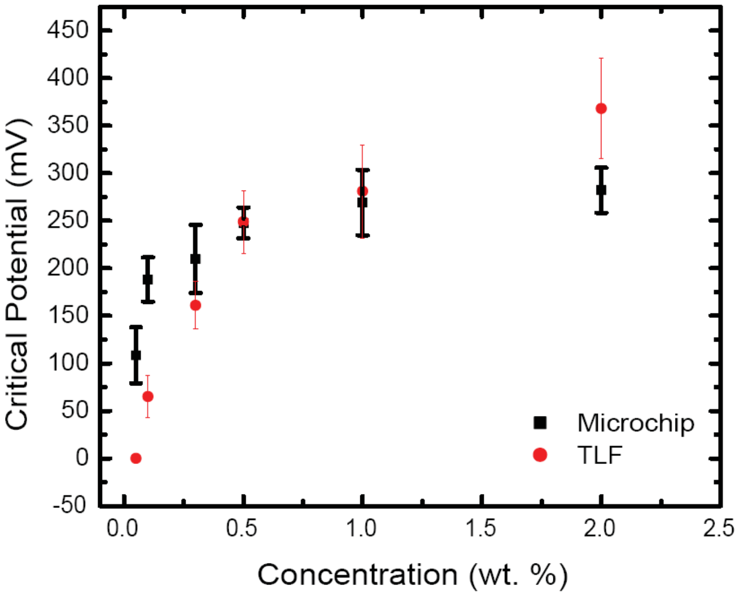

Figure 9.4.2. Comparison of critical potentials between TLF-PBT films (200 μm diameter) and microchip films (~13 μm diameter) for lecithin surfactant.

As in the case of porous plate cell experiments, the impact of concentration changes, which are in very narrow range, is clearly discernible on stability of microchip films. Thus, from the results of both methods, it is evident that the critical potential can resolve subtle differences of the adsorbed surfactant layer. The obtained values of critical potentials appear to be quite similar even for such two systems, that are distinguisheable by a great differences in film dimensions. This, again in turn, indicates that whatever is the mechanism of the electric stress-provoked film disintegration, it does not depend on film size.

## Chapter 10. Application of AC electric field

Figure 10.2 gives the dependence of calculated specific film capacitance for equilibrium films at different thicknesses. All experiments were performed with films having a diameter of 750 μm. It is seen from the Figure 10.2 that decrease in film thickness leads to linear increase in the specific film capacitance. Capacitance data were used for the calculation of the values of the relative film permittivity at each thickness. Thus the calculated relative film permittivity from all experiments appeared to be 5.2 ± 0.2. To our knowledge, no estimation of dielectric permittivity for water in oil emulsion thin liquid films has been reported in literature.

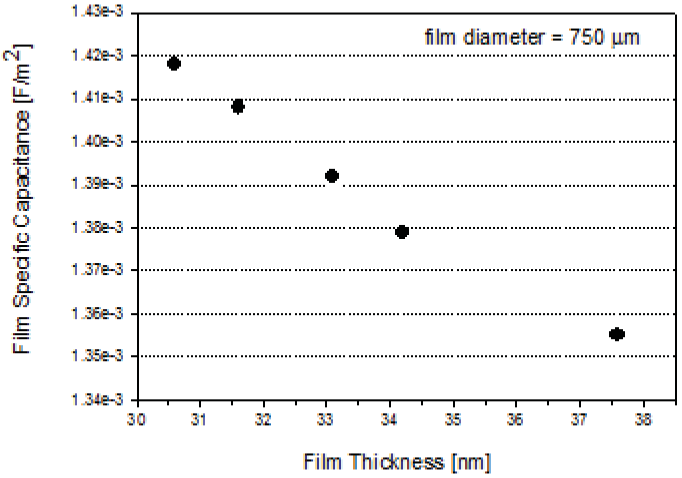

Figure 10.2. Dependence of specific film capacitance on equilibrium film thickness for 25 % diluted bitumen in toluene

In another set of experiments, films formed from 3% toluene solutions of asphaltenes were studied at two constant diameters, Figure 10.3.

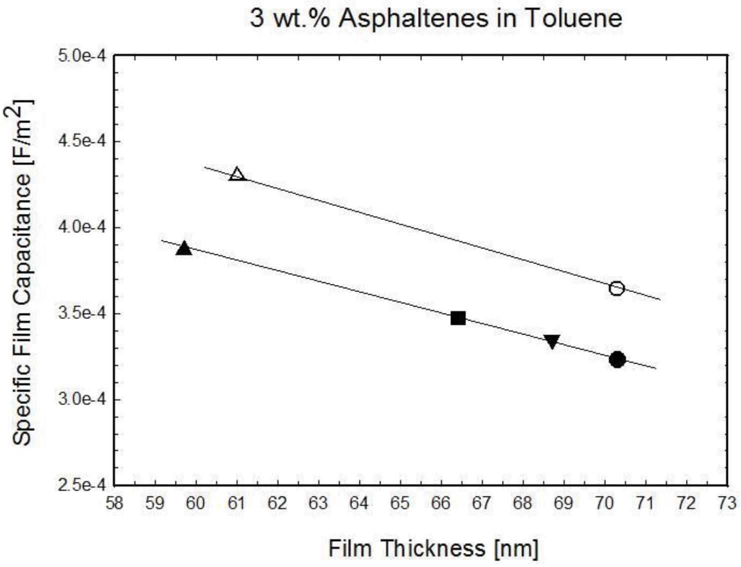

Figure 10.3. Specific film capacitance as a function of equilibrium thickness for 3wt% asphaltene stabilized films in toluene (film diameters are 500 μm and 400 μm for black and white symbols, respectively)

Thus, for films with diameter of 500 μm the value appeared to be 2.6, and for smaller films (400 μm) it is 2.95. The obtained disparity might be due to experimental artifacts and needs further elucidation.

## Main Contributions

1. **A new method for electro-microinterferometric studies of water-in-oil emulsion films is developed.** It is based on the existing thin liquid film – pressure balance technique (TLF-PBT). A modification of the Exerowa-Scheludko porous plate cell was implemented by adding electrodes as well as the upgradement of TLF-PBT. This allows combined application of AC or DC polarizations with the optical microinterferometry on emulsion films. The major advantage of the method is that within a single experiment and on the same film specimen, it is possible to determine independently the most important film parameters. Film thickness and corresponding rate of film drainage are obtained microinterferometrically, film diameter is monitored optically, critical voltage of rupture is measured directly, film capacitance is estimated from electrical impedance measurements. This provided experimental data for a straight forward calculation of the relative dielectic permittivity of w/o/w bitumen and asphaltenic emulsion film. So far, there has not been a

method that allows simultaneous investigation of film properties both optically and electrically.

2. **Critical voltages and critical electric field strengths for the film rupture were obtained.** Critical voltage apperas to be useful as a parameter describing film stability by showing its sensitivity to the surfactant concentration, to the type of surfactant, and to the type of the organic solvent.

   For the case of bitumen films in toluene, equilibrium thickness increased with increase of concentration. Obtained mean values of critical voltages as well as mean critical electric fields rose with concentration. Equilbrium bitumen films in heptane also get thicker with increase of concentration. These films show similar increase of critical voltages, however their mean critical field strengths are much higher than those for toluene-diluted films due to their overall smaller thicknesses. Unlike bitumen films, asphaltenic ones in toluene do not show increase of equilibrium thickness with concentration, but on a contrary. Measured mean critical voltages, their spread along with calculated mean critical fields show moderate increase of stability with asphaltenic concentration. Comparison of critical voltages between toluene-diluted bitumen and asphaltenic films, both having the same thickness (ca.45 nm) shows that asphaltenic films are much more stable despite their significantly lower concentration. Model lecithnin-stabilized films in toluene demonstrate that within the very narrow concentration range, there is a substantial increase of critical voltages with much less overlaping of scatered data. This is much pronounced difference in sensitivity of model system towards electro-induced rupture compared to complex bitumen and asphaltenic films.

   Stability measurements of bitumen and asphaltenic films within the film diameter range 200÷800 μm did not indicate a dependence on film size. Comparison of critical potentials between TLF-PBT films (200 μm diameter) and microchip films (~13 μm diameter) for lecithin surfactant further manifested lack of film size dependence.

3. **New type of isotherm, namely DC voltage-thickness isotherm, was introduced** and the corresponding electric field strength-thickness isotherm. After initial application of voltage ramps on Abil-stabilized equilibrium films, thickness remains the same. Further increase of voltage leads to sudden and sharp reduction of film thickness and loss of

stability. The corresponding voltage was named “threshold voltage for the onset of instability”. DC voltage-thickness isotherms allow also determination of critical thickness of rupture. Experiments show reasonable reproducibility of voltage-thickness curves, considering the stochastic nature of appearance of threshold instability and the final rupture. Generally speaking, higher the threshold voltages higher the critical values appear to be. There is no observable dependence of thickness-voltage isotherms on film size and on speed of applied voltage ramps. The influence of capillary (mechanical) pressure on voltage-thickness isotherms was investigated as well as its effect on critical thickness and critical voltage. With increase of capillary pressure the thickness of rupture decreases as well as the critical voltage.

4. Superimposition of constant DC voltage on capillary pressure-thickness isotherms enabled the **introduction of critical mechanical pressure at given DC voltage as another electro-mechanical stability parameter.** Increase of voltage shifts disjoining pressure isotherms towards lower thicknesses, and thus affecting the interfacial forces within the film. Overall trend for decrease of critical pressure with the DC field is noticeable.

5. **Experimental indications for the possible mechanisms of electric break-up were obtained.** Rupture of thick bitumen films occurs via formation of thin black spots at film periphery, while rupture of thin black bitumen films occurs via appearance of white thick spots within the entire film area. Different conductance behaviour (with and without current leakage) of the films prior to the rupture were demonstrated, hinting at different mechanisms of break-up. Application of alternating DC cycles with varying polarity manifested the reversibility of the appearance of film thinning-thickening instability patterns.

## List of publications included in the dissertation and noted citations

1. Panchev N., Khristov Khr., Czarnecki J., Exerowa D., Bhattacharjee S., Masliyah J., A new method for water-in-oil emulsion film studies, 2008, Colloids and Surfaces A: Physicochemical and Engineering Aspects, (1-3) 74-78, IF 4.539 (9 Citations)

2. Czarnecki J., Khristov K., Masliyah J., Panchev N., Taylor S.D., Tchoukov P., Application of Scheludko–Exerowa thin liquid film technique to studies of petroleum W/O emulsions, 2017, Colloids and Surfaces A: Physicochemical and Engineering Aspects, 2-10, IF 4.539 (9 Citations)

3. Panchev N., Khristov Khr., Czarnecki J., Electro-microinterferometric studies of water-in-oil emulsion films stabilized by natural and synthetic surfactants, Nanoscale Phenomena and Structures, edited by D.Kashchiev, prof.M.Drinov Publishing House, Sofia, 2008

## Dissertation materials presented in conferences

### Oral presentations

1. N.Panchev, Khr. Khristov, Jan Czarnecki, A New Method for Electro-Microinterferometric Studies: Development and Application, NPS (Nanoscale phenomena and structures in bulk and surface phases), Feb 26-Mar 02, 2008, Sofia, Bulgaria

2. F.Mostowfi, P.Tchoukov, N.Panchev, Khr.Khristov, T.Dabros, J.Czarnecki, Electrohydrodynamic Instabilities in Emulsion Films, 27 th ECIS conference, 1-6 September, 2013, Sofia, Bulgaria

3. N.Panchev, Khr.Khristov, J.Czarnecki, A New Method for Electro-Microinterferometric Studies of Water-in-Oil Emulsion Films: Development and Application with Natural and Synthetic Surfactants, 27 th ECIS conference, 1-6 September, 2013, Sofia, Bulgaria

4. N.Panchev, Khr. Khristov , Jan Czarnecki , A New Method for Electro-Optical Studies of Water-in-Oil Emulsion Films: Development and Application, 6th International Workshop on Bubble and Drop Interfaces, July 06-10, 2015 Potsdam/Golm, Germany

### Poster presentations

1. J.Czarnecki, D.Exerowa, Khr. Khristov, J.Masliyah, E.Musiał and N.Panchev, Investigations of Emulsion Films using Electrochemical Methodology, 79th ACS Colloid and Surface Science Symposium, Clarkson University, June 12-15, 2005, Potsdam, NY, USA.

2. N.Panchev, Khr. Khristov , Jan Czarnecki, D.Exerowa, A New Method for Electro-Microinterferometric Studies: Development and Application, NPCIS 2007, Plovdiv, Bulgaria

3. N.Panchev, Khr. Khristov , Jan Czarnecki, Electro-Microinterferometric Studies of Water-in-Oil Emulsion Films Stabilized by Natural and Synthetic Surfactant, NPS (Nanoscale phenomena and structures in bulk and surface phases), 26 Feb-02 March, 2008, Sofia, Bulgaria

4. N.Panchev, Khr.Khristov, J.Czarnecki, A New Method for Electro-Microinterferometric Studies of Water-in-Oil Emulsion Films, 27 th ECIS conference, 1-6 September, 2013, Sofia, Bulgaria

5. N.Panchev, Khr. Khristov, J.Czarnecki, A New Method for Electro-Microinterferometric Studies of Water-in-Oil Emulsion Films: Development and Application with Natural and Synthetic Surfactants, SGI-FunD Symposium, 29-31 October 2015, Sofia, Bulgaria